ARTICLES

Theoretical Study on the Thermal and Photochemical Isomerization Reactions of Dicyanoacetylene Complex of Platinum $Pt(PH_3)_2(C_4N_2)$

Hiromi Nakai,[†,‡] Sumihito Fukada,[†] and Hiroshi Nakatsuji*[,†,§]

Department of Synthetic Chemistry and Biological Chemistry, Faculty of Engineering, Kyoto University, Sakyo-ku, Kyoto 606-01, Japan, and Institute for Fundamental Chemistry, 34-4, Takano-Nishihiraki-cho, Sakyo-ku, Kyoto 606, Japan

Received: March 19, 1996; In Final Form: July 28, 1996[⊗]

The electronic mechanism of the photoisomerization of the dicyanoacetylene complex of platinum $Pt(PH_3)_2(C_4N_2)$ to the acetylide complex $Pt(PH_3)_2(CN)(C{\equiv}CCN)$ has been investigated theoretically. The geometries of the ground and excited states are optimized by the Hartree−Fock (HF) and single excitation configuration interaction (SE-CI) methods, respectively. In the thermal process, the decomposition reaction of $Pt(PH_3)_2(C_4N_2)$ into $Pt(PH_3)_2$ and C_4N_2 occurs preferentially but the association leads to the acetylene complex rather than to the acetylide complex. The reactant, transition state, and product all have planar structures. On the other hand, in the photochemical process, the dicyanoacetylene complex is isomerized smoothly into the acetylide complex. Neither the decomposition of $Pt(PH_3)_2(C_4N_2)$ into the neutral separated system $Pt(PH_3)_2 + C_4N_2$ nor that into the ionic separated systems $Pt(PH_3)_2^+ + C_4N_2^-$ and $Pt(PH_3)_2(C_4N_2)^+ + CN^-$ occurs. The intramolecular photoisomerization occurs through a bisect complex in the singlet excited state and a three-coordination Pt complex in the triplet state.

I. Introduction

Ever since the discovery of the Zeise's salt,[1,2] π-complexes of olefins on transition metals have presented various important chemical reactions.[3] For example, the catalytic activity of transition metal complexes in the aromatization or polymerization of acetylene hydrocarbons[4−6] is of particular interest. Isomerization from an acetylene to an acetylide complex shown below has been shown to be an important step in polymerization reactions.

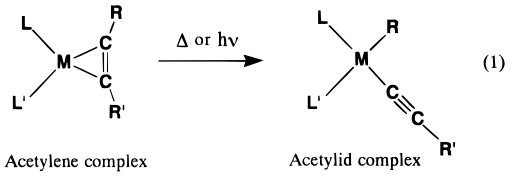

Acetylene complex Acetylid complex (1)

Although most polymerization reactions proceed thermally, that of the dicyanoacetylene complex of platinum cannot proceed without light irradiation,[7,8] and only the structure of the product has been reported experimentally.[7] Several aspects of this photochemical isomerization reaction need to be clarified: the role of photoirradiation, electronic states involved, reaction pathway, etc. So far, we have studied several photochemical processes of metal complexes[9,10] and metal surfaces[11,12] theoretically.

The main purpose of this study is to clarify theoretically the electronic processes of the photoisomerization reaction of the Pt dicyanoacetylene complex. We examine the electronic structures of several lower singlet and triplet states of the $Pt(PH_3)_2(C_4N_2)$ complex and determine the structures of the intermediates in this reaction using a geometry optimization procedure. We investigate the possibilities of both intermolecular and intramolecular isomerization reactions and the possibilities of thermal reactions.

II. Calculations

An experimental study on the photoisomerization reaction has been reported for $Pt(PPh_3)_2(C_4N_2)$.[7] Since the phenyl group is large and likely to have a minor role in this reaction, we take $Pt(PH_3)_2(C_4N_2)$ as a model compound for the present study.

The electronic structure of the singlet ground state of the Pt dicyanoacetylene complex is calculated by the ab initio restricted Hartree−Fock (RHF) method, and those of the singlet and triplet excited states are calculated by the single excitation configuration interaction (SE-CI) method. The structures of the reactant, product, intermediate, and transition state (TS) are determined by the energy gradient method. The calculations are performed using the Gaussian 92 program.[13]

The Gaussian bases for the Pt and P atoms are the (3s3p3d)/[3s2p2d] and (3s3p)/[2s2p] sets, respectively, replacing the Xe and Ne cores by the respective effective core potentials.[14,15] The (9s5p)/[4s2p] set of Huzinaga−Dunning is used for carbon and nitrogen, and the (4s)/[2s] set is used for hydrogen.[16]

III. Thermal Isomerization of $Pt(PH_3)_2(C_4N_2)$

In this section, we examine the thermal isomerization of $Pt(PH_3)_2(C_4N_2)$ in the ground state. First, we show the bonding between $Pt(PH_3)_2$ and C_4N_2 in the reactant $Pt(PH_3)_2(C_4N_2)$. Next, we examine the possibilities of the intramolecular and intermolecular isomerization reaction of $Pt(PH_3)_2(C_4N_2)$ in the

[†] Kyoto University.
[‡] Present address: Department of Chemistry, School of Science and Engineering, Waseda University, Tokyo 169, Japan.
[§] Institute for Fundamental Chemistry.
* Corresponding author.
[⊗] Abstract published in *Advance ACS Abstracts,* December 15, 1996.

S1089-5639(96)00830-4 CCC: $14.00

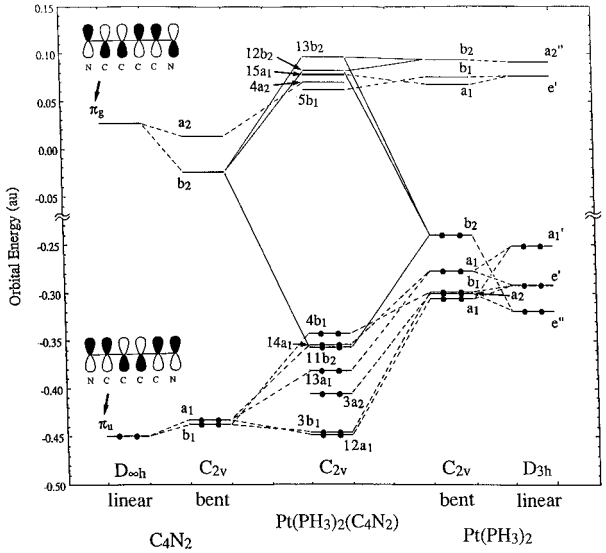

Figure 1. Orbital correlation diagram for the interaction of $Pt(PH_3)_2$ and C_4N_2 in the dicyanoacetylene Pt complex.

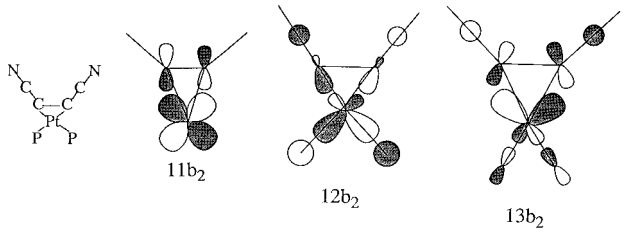

Figure 2. Schematic molecular orbital for the π bonding ($11b_2$) and the π antibonding ($12b_2$, $13b_2$) interactions between $Pt(PH_3)_2$ and C_4N_2.

ground state, which are shown in subsections III.B and III.C, respectively.

A. Interaction between $Pt(PH_3)_2$ and C_4N_2 in the Reactant. Figure 1 shows the orbital correlation diagram for the interaction of $Pt(PH_3)_2$ and C_4N_2 in the reactant $Pt(PH_3)_2(C_4N_2)$. Both $Pt(PH_3)_2$ and C_4N_2 fragments are linear in the free system, while they are bent in the interacting system. The highest occupied (HO) MO π_u and lowest unoccupied (LU) MO π_g of the linear C_4N_2 molecule have two and three nodes, respectively, as illustrated in Figure 1. The degenerate HOMO splits into a_1 and b_1 MOs and shifts to the higher energy side, and the LUMO splits into a_2 and b_2 MOs and shifts to the lower energy side. It is noted that the energy shift of the b_2 MO is largest. On the other hand, five MOs (e'', e', a_1', e', and a_2'') of the linear $Pt(PH_3)_2$ molecule shown in Figure 1 are all localized on Pt. The occupied e'', e', and a_1' MOs are mainly the (d_{xz}, d_{yz}), ($d_{x^2-y^2}$, d_{xy}), and (d_{z^2} + s) AOs of Pt, respectively, and the unoccupied e' and a_2'' MOs are mainly the (p_x, p_y) and p_z AOs of Pt, respectively. It is noted that a large energy shift is seen in the b_2 MO, which is the HOMO, of the bent $Pt(PH_3)_2$ molecule.

For the reactant, $12a_1$, $3b_1$, and $4a_2$ MOs mainly consist of the C_4N_2 orbitals, and $3a_2$, $13a_1$, $14a_1$, $4b_1$, $5b_1$, and $15a_1$ MOs consist of the $Pt(PH_3)_2$ orbitals. The interaction in the $11b_2$ MO contributes to the bonding between the $Pt(PH_3)_2$ and C_4N_2 fragments. As shown in Figure 2, this interaction corresponds to the π back-donation, which is more important than the σ donation. This result agrees with a nuclear magnetic resonance study.[17] Many studies have investigated the bonding in acetylene complexes of transition metals,[18−24] and the Pt(0) complex has been shown to be planar because of this π bond.[23,24] The $12b_2$ and $13b_2$ MOs are the antibonding orbitals for the $11b_2$ MO as shown in Figure 2.

B. Intramolecular Isomerization Reaction. We have performed geometry optimizations for the reactant, product, and transition state (TS) of the intramolecular isomerization reaction, keeping the C_s symmetry; the P−H distances and the PtPH angles were fixed at 1.41 Å and 117.69°, respectively. Next, we calculated the potential energy curves (PECs) of these three species as a function of the torsional angle between the $Pt(PH_3)_2$ and C_4N_2 as shown in Figure 3. Since all these species are stable at angle zero (Figure 3), the thermal reaction should proceed keeping a planar structure as follows:

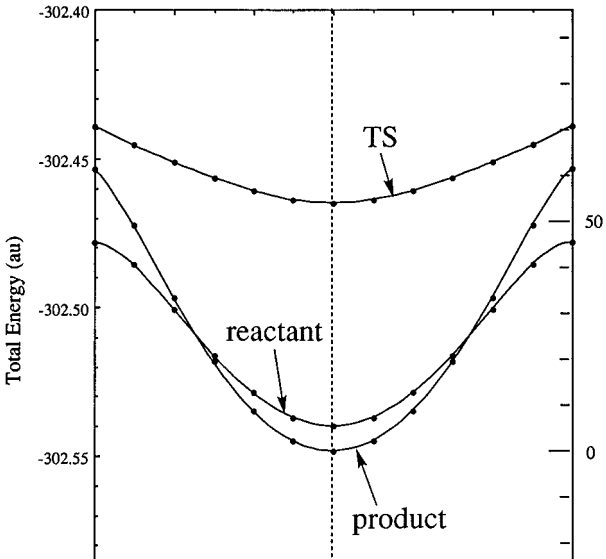

Figure 3. Potential energy curves for the torsion of the $Pt(PH_3)_2$ and C_4N_2 parts of the reactant, TS, and product in the ground state calculated by the HF method. The energy scale on the right-hand side is in kcal/mol relative to the energy of the product at an angle of 0°.

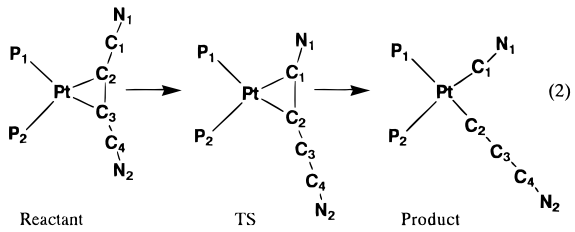

Table 1 shows the relative energies and the geometric parameters of these three species. The experimental data for the geometries of the reactant and product are due to $Pt(PPh_3)_2$-(PhCCPh) (ref 25) and $Pt(PPh_3)_2$(CN)(CCCN) (ref 7), respectively. The average discrepancies in the bond distance and angle are 0.10 Å and 4.7°, respectively. In the reaction shown in eq 2, the Pt−C3 and C1−C2 bonds are dissociated and the Pt−C1 bond is created. Thus, the C2 and C3 atoms are linked to the Pt atom in the reactant, while the C1 and C2 atoms are linked in the TS and product. In this regard, the TS structure resembles that of the product. On the other hand, for the C1−C2 distance the TS (1.577 Å) is closer to the reactant (1.404 Å) than to the product (2.874 Å).

C. Thermal Decomposition Reaction. We next investigate the possibility of the intermolecular isomerization reaction, i.e., the decomposition reaction in the ground state. Optimized geometries for the decomposition processes of the reactant and product into $Pt(PH_3)_2$ and C_4N_2 parts are shown in Figures 4 and 5, respectively. The distance R between Pt and the C2−C3 or C1−C2 bond is adopted for the reaction coordinate. The other parameters are optimized at each point except for the PH_3

TABLE 1: Relative Energies and Geometric Parameters of the Reactant, TS, and Product

system	relative energy[a] (kcal/mol)	bond distance (Å) term	RHF[b]	exptl	bond angle (deg) term	RHF[b]	exptl
reactant[c]	0.0	Pt−C2	2.120 (+0.06)	2.06	C2PtC3	35.39 (−4)	39
		Pt−C3	2.120 (+0.06)	2.06	P1PtP2	103.92 (+2)	102
		Pt−P1	2.491 (+0.21)	2.28	P1PtC2	110.34 (+1)	109
		Pt−P2	2.491 (+0.21)	2.28	P2PtC3	110.34 (+1)	109
		N1-C1	1.156		N1C1C2	180.00[e]	
		C1-C2	1.404		C1C2C3	146.47 (+6)	140
		C2-C3	1.289 (−0.03)	1.32	C2C3C4	146.47 (+6)	140
		C3-C4	1.404		C3C4N2	180.00[e]	
		C4-N2	1.156				
TS	+47.0	Pt−C1	2.189		C1PtC2	42.72	
		Pt−C2	2.139		P1PtP2	112.73	
		Pt−P1	2.517		P1PtC1	102.88	
		Pt−P2	2.495		P2PtC2	101.67	
		N1-C1	1.165		N1C1Pt	143.39	
		C1-C2	1.577		PtC2C3	147.80	
		C2-C3	1.218		C2C3C4	178.26	
		C3-C4	1.377		C3C4N2	180.00[e]	
		C4-N2	1.157				
product[d]	−5.3	Pt−C1	2.061 (+0.04)	2.02	C1PtC2	88.57 (+5.1)	83.5
		Pt−C2	2.056 (+0.10)	1.96	P1PtP2	96.99 (−4.8)	101.8
		Pt−P1	2.506 (+0.19)	2.32	P1PtC1	86.83 (+2.6)	84.2
		Pt−P2	2.499 (+0.17)	2.33	P2PtC2	87.61 (−2.9)	90.5
		N1-C1	1.160 (−0.01)	1.17	N1C1Pt	177.02 (+7.2)	169.8
		C1-C2	2.874 (+0.22)	2.65	PtC2C3	178.25 (+6.1)	172.2
		C2-C3	1.211 (−0.03)	1.24	C2C3C4	180.00[e] (−6.3)	173.7
		C3-C4	1.384 (+0.07)	1.31	C3C4N2	180.00[e] (+11.5)	168.5
		C4-N2	1.156 (−0.00)	1.16			
average discrepancy			(0.10)			(4.7)	

[a] Energy difference from the reactant. [b] Differences from experimental values are shown in parentheses. [c] Experimental data for the $Pt(PPh_3)_2(PhCCPh)$ complex are cited from ref 25. [d] Experimental data for the $Pt(PPh_3)_2(CN)(CCCN)$ complex are cited from ref 7. [e] These bond angles are fixed at 180° in the optimization calculations.

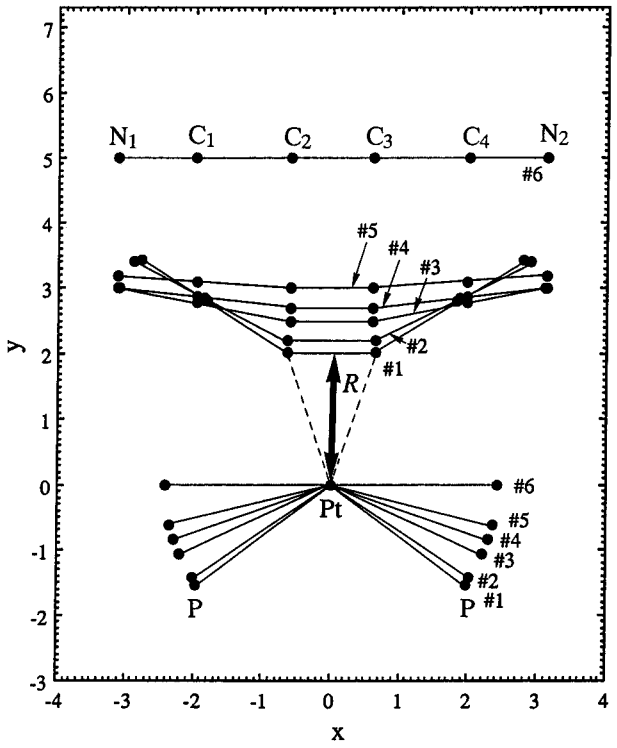

Figure 4. Optimized geometries for the decomposition process of the reactant. The distance *R* between Pt and the C2−C3 bond is adopted for the reaction coordinate. The positions of **1**−**6** correspond to R = 2.0198 (reactant), 2.2, 2.5, 2.7, 3.0, and 5.0 Å, respectively.

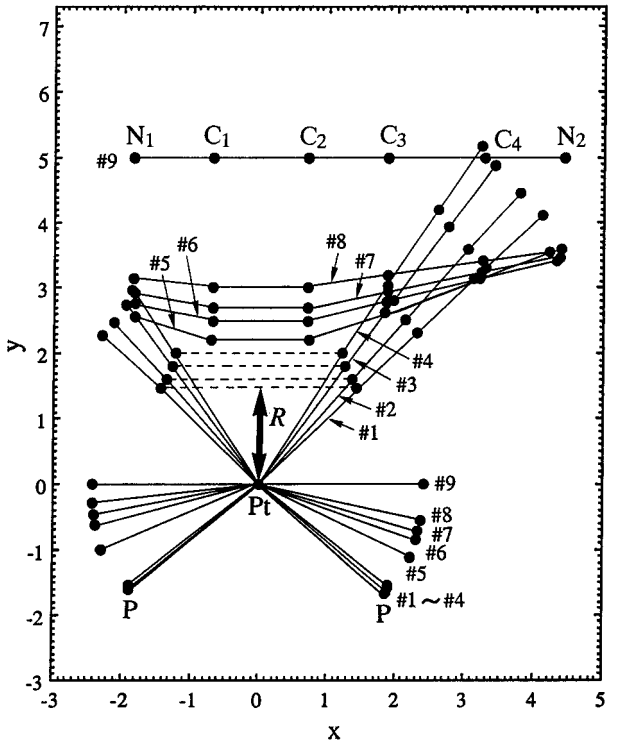

Figure 5. Optimized geometries for the decomposition process of the product. The distance *R* between Pt and the C1−C2 bond is adopted for the reaction coordinate. The positions of **1**−**9** correspond to R = 1.4748 (product), 1.6, 1.8, 2.0, 2.2, 2.5, 2.7, 3.0, and 5.0 Å, respectively.

part. In both processes, the $Pt(PH_3)_2$ and C_4N_2 parts become linear at a separation of 5 Å. The decomposition of the product includes the formation of the C1−C2 σ bond, which occurs around R = 2.0−2.2 Å. The geometries of the two P atoms do not change much up to R = 2.0 Å.

Figure 6 shows the PECs for the reaction pathways in Figures 4 and 5. The heats of the decompositions of the reactant and

TABLE 2: Singlet Ground and Excited States of $Pt(PH_3)_2(C_4N_2)$ with the Reactant Structure

state	excitation energy (eV)	main configuration[a] configuration[b]	character[c]	coefficient	oscillator strength
X^1A_1	0.00	HF		1.0000	
1^1A_2	4.18	$4b_1 \rightarrow 13b_2$	M → A	−0.5486	forbidden
		$4b_1 \rightarrow 12b_2$	M → A	0.3208	
1^1B_2	4.21	$14a_1 \rightarrow 13b_2$	M → A	−0.5201	0.0963
		$14a_1 \rightarrow 12b_2$	M → A	0.3292	
2^1B_2	4.82	$13a_1 \rightarrow 13b_2$	M → A	0.4872	0.7209
		$13a_1 \rightarrow 12b_2$	M → A	−0.3186	
1^1B_1	5.07	$3a_2 \rightarrow 13b_2$	M → A	−0.5555	0.0050
		$3a_2 \rightarrow 12b_2$	M → A	0.3570	
2^1A_2	5.11	$14a_1 \rightarrow 4a_2$	M → L	0.5384	forbidden
2^1B_1	5.50	$11b_2 \rightarrow 4a_2$	B → L	0.6464	0.3049

[a] Configurations whose CI coefficients (absolute values) are more than 0.3 are shown. [b] The symmetries of the MOs are shown in parentheses. [c] M, L, B, and A indicate the metal (Pt), ligand (C_4N_2), bonding, and antibonding between Pt and C_4N_2, respectively.

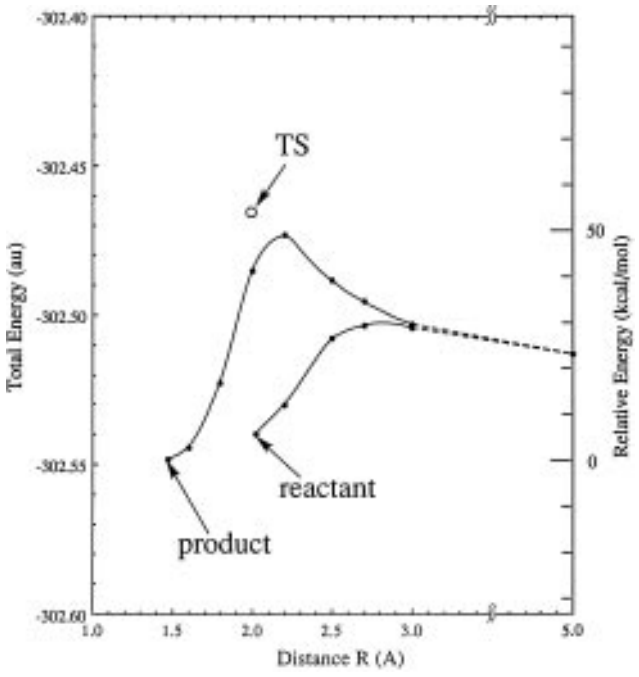

Figure 6. Potential energy curves for the decomposition processes of the reactant and product in the ground state calculated by the HF method. The geometries of these processes are shown in Figures 4 and 5. The circle indicates the energy level of the TS for the isomerization reaction. The energy scale on the right-hand side is in kcal/mol relative to the energy of the product.

the product are calculated to be 16.6 and 21.9 kcal/mol, respectively. The barriers of the two PECs are quite different: 22.8 kcal/mol for the reactant and 47.0 kcal/mol for the product, which means that the association barriers are 6.2 and 25.2 kcal/mol, respectively. The high barrier of the latter process is due to the breaking of the Pt−C1 and Pt−C2 bonds and the formation of the C1−C2 bond.

Since the energy level of the TS for the intramolecular isomerization of eq 2, which is marked by the circle in Figure 6, is higher than the barrier for the decomposition of the reactant, the decomposition reaction occurs more easily than the isomerization reaction. Furthermore, the association of the $Pt(PH_3)_2$ and C_4N_2 parts leads to the reactant rather than the product. Therefore, the isomerization reaction does not proceed thermally.

IV. Photochemical Isomerization of $Pt(PH_3)_2(C_4N_2)$.

In this section, we study the photochemical isomerization of $Pt(PH_3)_2(C_4N_2)$. The photochemical reaction starts with the absorption of light by the reactant. In subsection IV.A, we show the nature of the singlet excited states of the reactant and we further examine the possibility of the decomposition in the excited states. Next, we examine the geometry relaxations in the singlet and triplet excited states, which are important for determining the reaction pathway of the photochemical isomerization. They are shown in subsections IV.B and IV.C, respectively. In subsection IV.D, we study the product-formation process and give a brief summary of the photoisomerization reaction.

A. Photoabsorption of the Reactant. First, we calculate the singlet excited states of $Pt(PH_3)_2(C_4N_2)$ in the reactant geometry by the HF/SE-CI method. Table 2 shows the excitation energy, the main configuration, and the oscillator strength for the singlet excited states below 5.50 eV. As mentioned before, the $4b_1$, $14a_1$, $13a_1$, and $3a_2$ MOs are localized on the d and s AOs of Pt, and the $12b_2$ and $13b_2$ MOs are the π antibonding orbitals between the $Pt(PH_3)_2$ and C_4N_2 fragments. Therefore, the lower four excited states, 1^1A_2, 1^1B_2, 2^1B_2, and 1^1B_1, are due to the excitations from the metal to the antibonding orbitals. The bonding between $Pt(PH_3)_2$ and C_4N_2 should be weakened in these excited states.

Figure 7 shows the PECs of the decomposition into $Pt(PH_3)_2$ and C_4N_2 in the lower singlet and triplet states. Parts a and b of Figure 7 correspond to the decomposition from the planar and bisect forms, respectively. The bisect form is led by the torsion of the $Pt(PH_3)_2$ and C_4N_2 parts as discussed in section IV.B. The geometries used in these calculations are the same as those shown in Figure 4 except for the torsional angle between $Pt(PH_3)_2$ and C_4N_2. Both figures indicate that the singlet and triplet excited states do not lead to the decomposition. As shown in Figure 7b, the decomposition of the bisect form can proceed in the ground state. However, the recombination in the ground state does not lead to the isomerization product as shown in Figure 6.

The 2^1A_2 excited state lying at 5.11 eV is due to the electron-transfer excitation, M → L. Figure 8 shows the energy levels and the optimized geometries of the ionic systems, $Pt(PH_3)_2^+ + C_4N_2^-$ and $Pt(PH_3)_2(CCCN)^+ + CN^-$, in comparison with the ground and excited states of the reactant. The geometries are optimized at the HF level. These ionic separated systems lie at 5.99 and 7.16 eV, respectively, above the ground state of the reactant, which are also higher than the 2^1A_2 state of the reactant. In fact, the photon energy of the sun lamp used in the photoisomerization experiment[7] is 3−5 eV. Therefore, the ionic separated systems shown in Figure 8 do not exist as an intermediate of the photochemical isomerization reaction.

B. Relaxation in the Singlet Excited States. Since the photoexcited complex does not seem to decompose as studied above, the photochemical isomerization proceeds as the intramolecular reaction. Here, we examined the geometry relaxation of the complex in the singlet excited states. Figure 9 shows the PECs for the torsion between the $Pt(PH_3)_2$ and C_4N_2

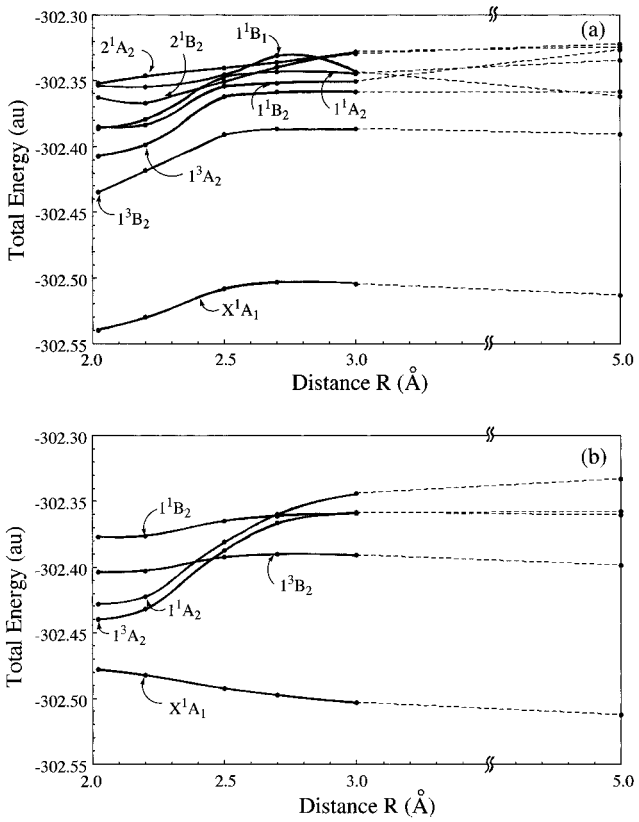

Figure 7. Potential energy curves for the decomposition process of the planar reactant (a) and the bisect form (b) in the singlet and triplet excited states compared with the ground-state process calculated by the HF/SE-CI method. The geometries shown in Figure 4 is adopted for the calculations.

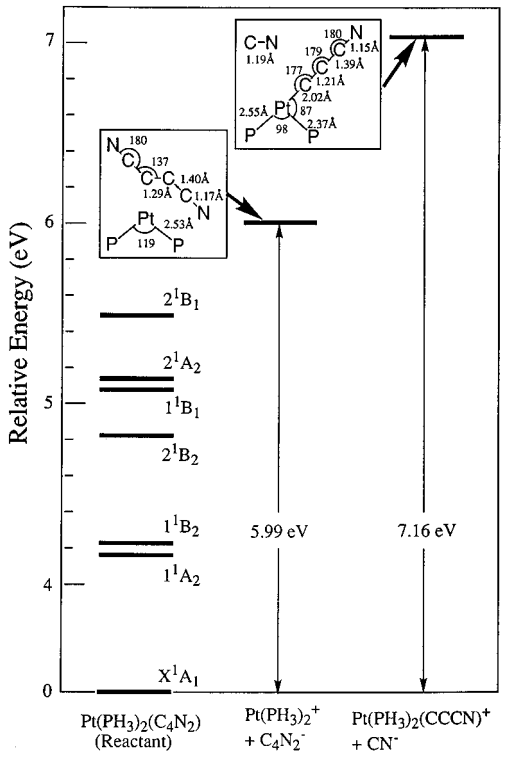

Figure 8. Energy levels and the optimized geometries for the ionic separated systems, $Pt(PH_3)_2^+ + C_4N_2^-$ and $Pt(PH_3)_2(CCCN)^+ + CN^-$, in comparison with the ground and excited states of the reactant calculated by the HF/SE-CI method.

parts of the reactant in the excited states compared with that of the ground state: the latter is the same as the PEC shown in

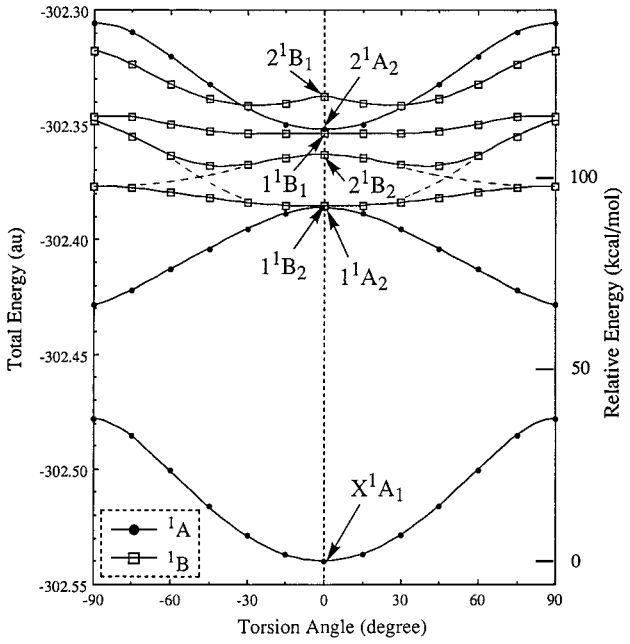

Figure 9. Potential energy curves for the torsion of the $Pt(PH_3)_2$ and C_4N_2 parts of the reactant in the singlet excited states compared with the ground-state process calculated by the HF/SE-CI method. The energy scale on the right-hand side is in kcal/mol relative to the energy of the ground state at an angle of 0°.

Figure 3. In the ground state, the molecule is stable at the planar geometry (torsional angle zero), but in the lowest excited state 1^1A_2 (2^1A), it is stable at the bisect form (90°). The curve of the 1^1B_2 state is nearly flat in comparison with those of the X^1A_1 and 1^1A_2 states and has a minimum at the planar structure. On the other hand, the curve of the 2^1B_2 state, which has the largest oscillator strength among the excited states below 5.50 eV, has a minimum near 45°. This minimum is due to the avoided crossing with the 1^1B_2 curve; namely, the 1^1B_2 states of the bisect form has the same nature as the 2^1B_2 state of the planar form. Therefore, the excitation to the 2^1B_2 state of the reactant structure leads to the bisect structure.

We further optimize the geometries of the planar and bisect dicyanoacetylene Pt complex in the 1^1A_2 and 1^1B_2 states. Table 3 shows the results. The stabilized energies by the optimization are calculated to be 13.6, 3.6, and 13.9 kcal/mol for the planar and bisect 1^1A_2 states and the planar 1^1B_2 state, respectively. For these three states, the maximum differences in the bond distance and the bond angle are +0.253 and −12.59, respectively, which shows that the effect of the excitation is not large. On the other hand, the bisect form of the 1^1B_2 state is much stabilized (23.4 kcal/mol). This is mainly due to the relaxation of the PPtP angle; namely, it is calculated to be 169.48° and about 65° larger than that of the reactant in the ground state.

C. Relaxation in the Triplet States. Since the isomerization reaction of eq 2 involves the dissociation of the Pt−C3 bond and the formation of the Pt−C1 bond with the Pt−C2 bond intact, we examine the three-coordination Pt complex in which the Pt atom is bonded to the C2 and two P atoms. Figure 10 shows the energy levels of the lower singlet and triplet states of the three-coordination Pt complexes, **4**−**6**. Complexes **1**, **7**, and **8** are the reactant, TS, and product, respectively. Complexes **2** and **3** correspond to the above-mentioned bisect complexes of the reactant, and the difference between them is the PPtP angle. The schematic structures of the complexes **1**−**8** are also shown in Figure 10.

For the lowest triplet state, the optimized geometry with the bisect structure corresponds to **4** and those with planar structures

TABLE 3: Total Energies and Optimized Geometric Parameters of the Planar and Bisect Dicyanoacetylene Pt Complexes in the 1^1A_2 and 1^1B_2 States

		bond distance (Å)		bond angle (deg)	
state	total energy (au)	term	value[a]	term	value[a]
1^1A_2	−302.407766	Pt−C2, Pt−C3	2.175 (+0.055)	C2PtC3	38.43 (+3.04)
(planar)	(−13.6)[b]	Pt−P1, Pt−P2	2.712 (+0.221)	P1PtP2	102.00 (−1.92)
		C2−C3	1.360 (+0.071)	C1C2C3, C2C3C4	133.88 (−12.59)
		C1−C2, C3−C4	1.415 (+0.011)	N1C1C2, C3C4N2	180.00[c]
		C1−N1, C4−N2	1.159 (+0.003)		
1^1A_2	−302.434206	Pt−C2, Pt−C3	2.173 (+0.053)	C2PtC3	37.31 (+1.92)
(bisect)	(−3.6)[b]	Pt−P1, Pt−P2	2.534 (+0.043)	P1PtP2	98.83 (−5.09)
		C2−C3	1.324 (+0.035)	C1C2C3, C2C3C4	139.03 (−7.44)
		C1−C2, C3−C4	1.409 (+0.005)	N1C1C2, C3C4N2	180.00[c]
		C1−N1, C4−N2	1.158 (+0.002)		
1^1B_2	−302.407401	Pt−C2, Pt−C3	2.210 (+0.090)	C2PtC3	35.07 (−0.32)
(planar)	(−13.9)[b]	Pt−P1, Pt−P2	2.744 (+0.253)	P1PtP2	95.84 (−8.08)
		C2−C3	1.332 (+0.043)	C1C2C3, C2C3C4	136.50 (−9.97)
		C1−C2, C3−C4	1.416 (+0.012)	N1C1C2, C3C4N2	180.00[c]
		C1−N1, C4−N2	1.159 (+0.003)		
1^1B_2	−302.414301	Pt−C2, Pt−C3	2.266 (+0.146)	C2PtC3	33.64 (−1.75)
(bisect)	(−23.4)[b]	Pt−P1, Pt−P2	2.481 (−0.010)	P1PtP2	169.48 (+65.56)
		C2−C3	1.312 (+0.023)	C1C2C3, C2C3C4	138.98 (−7.49)
		C1−C2, C3−C4	1.411 (+0.007)	N1C1C2, C3C4N2	180.00[c]
		C1−N1, C4−N2	1.159 (+0.003)		

[a] Differences from the planar $Pt(PH_3)_2(C_4N_2)$ complex in the ground state are shown in parentheses. [b] The values in parentheses are the energy differences between the fixed and the optimized geometries. [c] These bond angles are fixed at 180° in the optimization calculations.

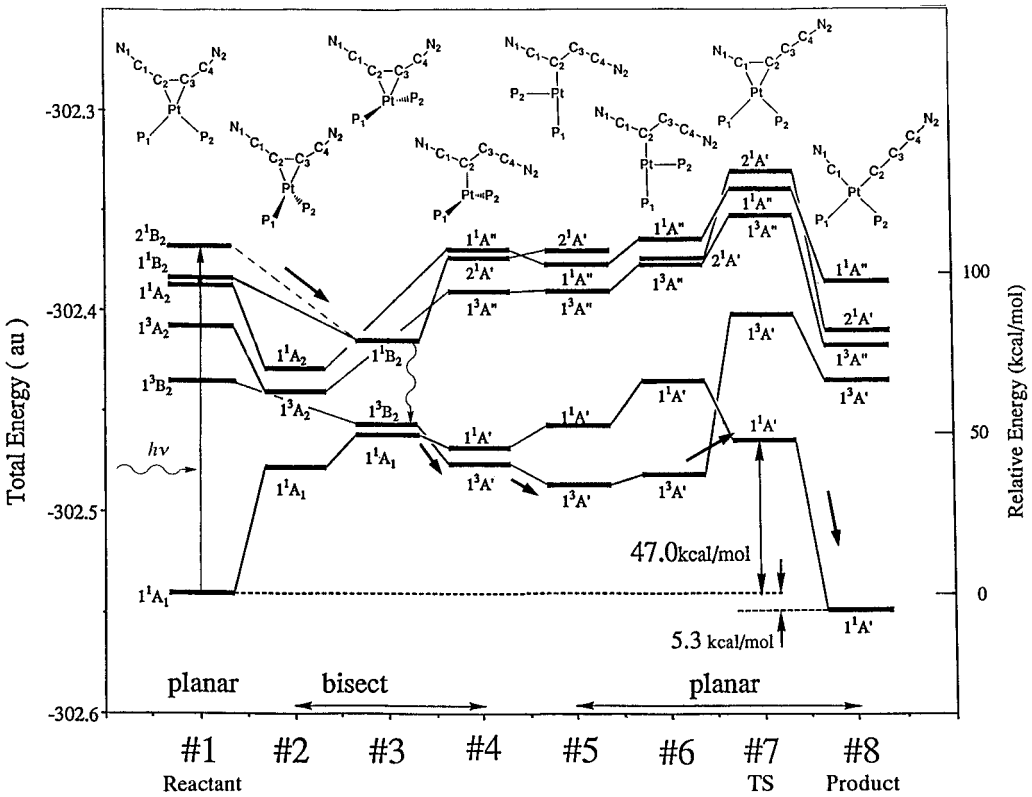

Figure 10. Energy diagram of the lower singlet and triplet states of $Pt(PH_3)_2(C_4N_2)$ for the photochemical isomerization reaction. The schematic structures of complexes **1**−**8** are shown in this figure.

to **5** and **6**. The main difference between **5** and **6** lies in the two phosphines bonded to Pt. In **4**−**6**, C_4N_2 is a trans-bent structure, which is similar to the stable structures of free acetylene derivatives in the lowest triplet state. Two spins are mainly located on Pt and C3; for example, in the **4** complex, the spin populations of Pt, C3, and C2 are 0.87, 0.80, and 0.14, respectively.

From **2** or **3** to **4**, the energy levels of the 1^3A_2, 1^1A_2, and 1^1B_2 states rise up and only the energy level of the 1^3B_2 state goes down. Namely, the transition to the 1^3B_2 state leads to the three-coordination Pt complex. This difference is related to the singlet−triplet separation. The energy difference between the 1^1B_2 and 1^3B_2 states at **4** (2.81 eV) is much larger than that between the $2^1A'$ and $1^3A'$ states at **3** (1.14 eV). (Note that the $1^1A'$ state is the closed-shell system.) Large energy differences also exist at **5** and **6**. Those in the A_2 and A'' states are 0.32 and 0.49 eV at **2** and **4**, respectively, of which the difference is only 0.18 eV.

D. Formation of the Product. The final step of the photoisomerization reaction is the relaxation to the lowest singlet state and the formation of the product. The **5** and **6** complexes represent different stable structures in the triplet state. These

triplet states are actually the ground state and are lower than those of the lowest singlet states. However, the complex in these states has an excess energy within the internal motions, since it is led from the 1^1B_2 state of the reactant (**1**). Therefore, the intersystem transition from the triplet to the lowest singlet states can occur with the excess energy and the product can be formed over the barrier in the lowest singlet state. It is noted that the reaction pathway through **5** or **6** is possible only for the photochemical reaction, since the energy levels of the lowest singlet states at **5** and **6** are higher than that of the TS (**7**) in the thermal reaction. By comparison of **5** and **6**, the two spins are located at Pt and C3 and the lobes of the SOMO at Pt extend in opposite directions because of the geometries of the two phosphines. Therefore, the **5** and **6** forms may easily lead to the reactant and the product, respectively.

From the above results, we conclude that the photoisomerization reaction proceeds according to the following sequence: (1) electronic transition to the singlet excited state (2^1B_2) by photoirradiation; (2) geometry relaxation to the bisect Pt complex in the singlet excited state (1^1B_2 in **3**); (3) intersystem crossing from the singlet excited state to the triplet state ($1^1B_2 \rightarrow 1^3B_2$ in **3**); (4) geometry relaxation to the three-coordination Pt complexes in the triplet state (**4**−**6**); (5) intersystem transition from the triplet state to the lowest singlet state, crossing over the TS of the singlet state; (6) formation of the product along the lowest singlet state curve.

V. Conclusions

We have studied the mechanism and the pathway of the photoisomerization reaction of $Pt(PH_3)_2(C_4N_2)$ by the ab initio MO theory using the HF and SE-CI methods.

The thermal reaction proceeds, maintaining a planar (C_s) structure, and the energy barrier is calculated to be 47.0 kcal/mol. This barrier is much higher than the barrier (22.8 kcal/mol) and the heat (16.6 kcal/mol) of the decomposition into $Pt(PH_3)_2$ and C_4N_2 fragments. The association of the separated system mainly produces the acetylene complex rather than the acetylide complex. Therefore, the isomerization reaction of $Pt(PH_3)_2(C_4N_2)$ to $Pt(PH_3)_2(CN)(CCCN)$ cannot proceed as a thermal process.

On the other hand, in the lower singlet excited states, 1^1A_2 and 1^1B_2, the bisect structures are more stable than the planar one. The Pt−C3 bond, which does not exist in the product, is still kept in these singlet excited states. Only the triplet 1^3B_2 ($1^3A'$) state gives the three-coordination Pt intermediate in which two phosphines and one C atom of C_4N_2 are bonded to Pt, while the triplet 1^3A_2 ($1^3A''$) state cannot. The intermediate in the triplet state is important for this photoisomerization reaction, and this notion should be confirmed by experiments based on the solvent effect with heavy atoms, which makes the transition from the singlet to the triplet states easier. The final step of the photoisomerization reaction is the transition from the lowest triplet to the lowest singlet state in the three-coordination Pt intermediate, where the complex has enough energy to pass into the TS.

The reaction mechanism, the reaction pathway, and the electronic mechanism clarified by the present ab initio study may be useful for the design of additional experiments on both the thermal and photochemical isomerization of Pt acetylene complexes.

Acknowledgment. All calculations were performed using the computers at the Data Processing Center of Kyoto University and the Institute for Molecular Science. Part of this study was supported by a Grant-in-Aid for Scientific Research from the Japanese Ministry of Education, Science, and Culture and by the New Energy and Industrial Technology Development Organization (NEDO).

TABLE 4: Total Energies of the Reactant, TS, and Product Calculated by the HF and SAC Methods

total energy (hartree) system	HF	SAC	correlation energy (hartree)
reactant (**1**)	−302.53985 (0.0)	−302.87150 (0.0)	−0.33165
TS (**7**)	−302.46493 (+47.0)	−302.73152 (+87.8)	−0.26659
product (**8**)	−302.54830 (−5.3)	−302.86390 (+4.8)	−0.31560

[a] Differences from the reactant are shown in parentheses (in kcal/mol).

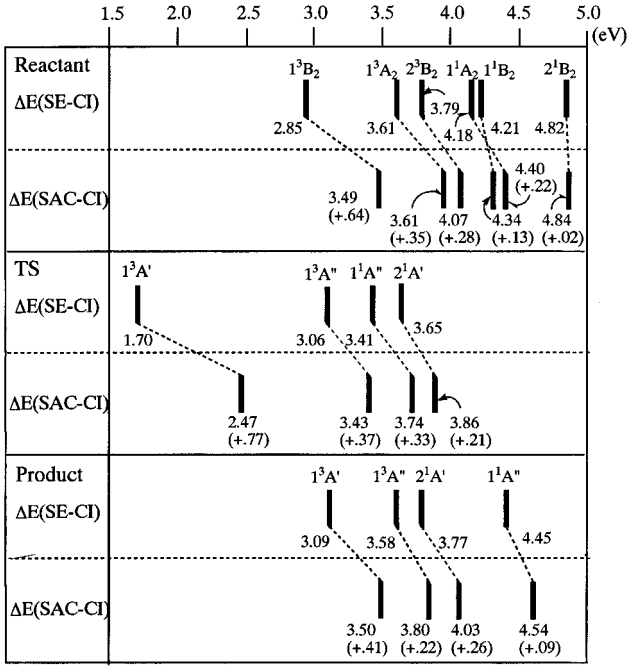

Figure 11. Comparison of the singlet and triplet excitation energies of the reactant, TS, and product calculated by the HF/SE-CI and SAC/SAC-CI methods.

Appendix: Accuracy of the Present Method

We show here the accuracy of the present method and the effects of electron correlations. We calculate the singlet and triplet states of the reactant (**1**), TS (**7**), and product (**8**) by the SAC/SAC-CI method.[26−28] The geometries optimized in the HF level are used. The active space of the SAC/SAC-CI calculations includes the higher 26 occupied MOs and the lower 68 unoccupied MOs obtained by the HF method. The energy threshold of 5.0×10^{-5} hartree is used to select the linked configuration state functions.[29] The program system SAC85 is used for the SAC/SAC-CI calculations.[30]

Table 4 shows the total energies of the three species (**1**, **7**, and **8**) calculated by the HF and SAC methods. The electron correlations are not so small in the ground state of these species. In particular, the electron correlations of **1** are larger than the others. This leads to the higher barrier and smaller heat of reaction. In fact, the isomerization reaction is calculated to be a little bit exothermic and endothermic by the HF and SAC methods, respectively. However, these results by the SAC calculations emphasize that the thermal isomerization reaction cannot occur, which is one of the conclusions based on the HF calculations.

Figure 11 shows the singlet and triplet excitation energies of the reactant, TS, and product calculated by the HF/SE-CI and

SAC/SAC-CI methods. We see that all the excitation energies obtained by the HF/SE-CI calculations are lower than those by the SAC/SAC-CI. This shows that the electron correlations in the ground state of the three complexes are larger than those in the excited states. The average and maximum differences of the excitation energies by both methods are 0.31 and 0.77 eV, respectively. It is noted that the orderings of the excited states are the same by both methods except for the 1^1A_2 and 1^1B_2 states of the reactant.

Thus, although the electron correlations work a little bit better in the ground state than in the excited states, the inclusion of the electron correlations never leads to a different mechanism for the thermal and photochemical isomerization reactions of $Pt(PH_3)_2(C_4N_2)$ in comparison with the HF/SE-CI results given in the text.

References and Notes

(1) Zeise, W. C. *Mag. Pharm.* **1830**, *35*, 105.
(2) Zeise, W. C. *Poggendorf's Ann. Phys.* **1827**, *9*, 632.
(3) Hartley, F. R. *Chem. Rev. (Washington, D.C.)* **1969**, *69*, 799.
(4) Meriwether, L. S.; Colthup, E. C.; Kennerly, G. W.; Reusch, R. N. *J. Org. Chem.* **1961**, *26*, 5155.
(5) Meriwether, L. S.; Leto, M. F.; Colthup, E. C.; Kennerly, G. W. *J. Org. Chem.* **1962**, *27*, 3930.
(6) Furlani, A.; Collamati, I.; Sartori, G. *J. Organomet. Chem.* **1969**, *17*, 463.
(7) Baddley, W. H.; Panattoni, C.; Bandoli, G.; Clemente, D. A.; Belluco. U. *J. Am. Chem. Soc.* **1971**, *93*, 5590.
(8) McClure, G. L.; Baddley, W. H. *J. Organomet. Chem.* **1970**, *25*, 261.
(9) Nakai, H.; Nakatsuji, H.; *J. Mol. Structure: THEOCHEM* **1994**, *311*, 141. Nakai, H.; Ohmori, Y.; Nakatsuji, H. *J. Phys. Chem.* **1995**, *99*, 8550.
(10) Hada, M.; Imai, Y.; Hidaka, M.; Nakatsuji, H. *J. Chem. Phys.* **1995**, *103*, 6993.
(11) Nakai, H.; Nakatsuji, H. *J. Chem. Phys.* **1995**, *103*, 2286.
(12) Nakatsuji, H.; Morita, H.; Nakai, H.; Murata, Y.; Fukutani, K. *J. Chem. Phys.* **1996**, *104*, 714.
(13) Frish, M. J.; H-Gordon, M.; Trucks, G. W.; Foresman, J. B.; Schlegel, H. B.; Raghavachari, K.; Robb, M. A.; Binkley, J. S.; Gonzalez, C.; Defrees, D. J.; Fox, D. J.; Whiteside, R. A.; Seeger, R.; Melius, C. F.; Baker, J.; Martin, R. L.; Kahn, L. R.; Stewart, J. J. P.; Topiol, S.; Pople, J. *Gaussian 92*; Gaussian, Inc.: Pittsburgh, PA, 1992.
(14) Hay, P. J.; Wadt, W. R. *J. Chem. Phys.* **1985**, *82*, 299.
(15) Wadt, W. R.; Hay, P. J. *J. Chem. Phys.* **1985**, *82*, 284.
(16) Huzinaga, S. *J. Chem. Phys.* **1965**, *42*, 1293. Dunning, T. H., Jr. *J. Chem. Phys.* **1970**, *53*, 2823.
(17) Koie, Y.; Shinoda, S.; Saito, Y. *J. Chem. Soc., Dalton Trans.* **1981**, 1082.
(18) Chatt, J.; Rowe, G. A.; Williams, A. A. *Proc. Chem. Soc., London* **1957**, 208.
(19) Chatt, J.; Duncanson, L. A.; Guy, R. G. *Chem. Ind. (London)* **1959**, 430.
(20) Chatt, J.; Duncanson, L. A.; Guy, R. G. *J. Chem. Soc.* **1961**, 827.
(21) Chatt, J.; Guy, R. G.; Duncanson, L. A. *J. Chem. Soc.* **1963**, 5170.
(22) Greaves, E. O.; Lock, C. J. L.; Maitlis, P. M. *Can. J. Chem.* **1968**, *46*, 3880.
(23) Wheelock, K. S.; Nelson, J. H.; Cusachs, L. C.; Jonassen, H. B. *J. Am. Chem. Soc.* **1970**, *92*, 5110.
(24) Nelson, J. H.; Jonassen, H. B. *Coord. Chem. Rev.* **1971**, *6*, 27.
(25) Glanville, J. O.; Stewart, J. M.; Grim, S. O. *J. Organomet. Chem.* **1967**, *7*, 9.
(26) Nakatsuji, H.; Hirao, K. *J. Chem. Phys.* **1978**, *68*, 2035.
(27) Nakatsuji, H. *Chem. Phys. Lett.* **1978**, *59*, 362; **1979**, *67*, 329, 334.
(28) Nakatsuji, H. *Acta Chim. Hung.* **1992**, *129*, 719.
(29) Nakatsuji, H. *Chem. Phys.* **1983**, *75*, 425.
(30) Nakatsuji, H. *Program System for SAC and SAC−CI Calculations*; Program Library No. 146 (Y4/SAC); Data Processing Center of Kyoto University: Kyoto, 1985; Program Library SAC85, No. 1396; Computer Center of the Institute for Molecular Science: Kyoto, 1981.